| | |
|---|---|
| ***Publication Year*** | 2017 |
| ***Acceptance in OA@INAF*** | 2020-09-09T14:16:38Z |
| ***Title*** | Sputtering of sodium and potassium from nepheline: Secondary ion yields and velocity spectra |
| ***Authors*** | Martinez, R.; Langlinay, Th.; Ponciano, C. R.; da Silveira, E. F.; PALUMBO, Maria Elisabetta; et al. |
| ***DOI*** | 10.1016/j.nimb.2017.01.042 |
| ***Handle*** | http://hdl.handle.net/20.500.12386/27254 |
| ***Journal*** | NUCLEAR INSTRUMENTS & METHODS IN PHYSICS RESEARCH. SECTION B, BEAM INTERACTIONS WITH MATERIALS AND ATOMS |
| ***Number*** | 406 |

# Sputtering of sodium and potassium from nepheline: secondary ion yields and velocity spectra

R. Martinez[1,2], Th. Langlinay[1], C.R. Ponciano[3], E.F. da Silveira[3], M.E. Palumbo[4], G. Strazzulla[4], J.R. Brucato[5], H. Hijazi[6], A.N. Agnihotri[1], P. Boduch[1], A. Cassimi[1], A. Domaracka[1], F. Ropars[1], H. Rothard[1,]*

[1] *Centre de Recherche sur les Ions, les Matériaux et la Photonique*

*Normandie Univ, ENSICAEN, UNICAEN, CEA, CNRS, CIMAP, 14000 Caen, France*

[2] *Departamento de Física, Universidade Federal do Amapá, Brazil*

[3] *Departamento de Física, Pontifícia Universidade Católica do Rio de Janeiro, Brazil*

[4] *INAF-Osservatorio Astrofisico di Catania, Italy*

[5] *INAF-Osservatorio Astrofisico di Arcetri, Firenze, Italy*

[6] *Université Aix-Marseille, France*

*rothard@ganil.fr

## ABSTRACT

Silicates are the dominant surface material of many Solar System objects, which are exposed to ion bombardment by solar wind ions and cosmic rays. Induced physico-chemical processes include sputtering which can contribute to the formation of an exosphere. We measured sputtering yields and velocity spectra of secondary ions ejected from nepheline, an aluminosilicate thought to be a good analogue for Mercury's surface, as a laboratory approach to understand the evolution of silicate surfaces and the presence of Na and K vapor in the exosphere. Experiments were performed with highly charged ion beams (keV/u - MeV/u) delivered by GANIL using an imaging XY-TOF-SIMS device under UHV conditions. The fluence dependence of sputtering yields gives information about the evolution of surface stoichiometry during irradiation. From the energy distributions N(E) of sputtered particles, the fraction of particles which could escape from the gravitational field of Mercury, and of those falling back and possibly contributing to populate the exosphere can be roughly estimated.

**Keywords:** Nepheline, Mercury, Sputtering, heavy Ions, Highly charged ions

## 1. INTRODUCTION

Among the three main classes of solid materials in space (ices, silicates and carbon-based ones), silicates are the most abundant and present throughout the Solar System and the interstellar medium [1]. Silicates are materials with a large diversity in chemical composition and structural properties and play an important function in the cosmic life cycle of matter [2]. In several silicates as it is the case of nepheline, the Si atom is coordinated in a tetrahedron by four O atoms, and different structures are formed linking the radical $[SiO_4]^{4-}$ with different atoms which should compensate the negative charge. Silicates are found both in amorphous and crystalline phases [3].

In the Solar System, silicates are present in planets and their moons [4], in transneptunian objects, in asteroids and meteorites, and in comets [5,6]. Silicates are the dominant component at Mercury's crust, even more abundant than iron. Sputtered particles can contribute to the formation of Mercury's active exosphere. The particle environment surrounding Mercury is complex and composed by i) thermal and directional neutral atoms originating via surface release and charge-exchange processes, and ii) ionized particles originating from photo-ionization and from surface release processes such as ion induced sputtering. Indeed, sputtering of the components of minerals present at the surfaces of Mercury and the Moon appears to be the most efficient source of sodium and potassium in their exosphere [7]. $Na^+$ and $K^+$ ions have been observed in Mercury's exosphere by the Messenger spacecraft [8].

Ion irradiation of solids can lead to physico-chemical changes. Among them are structural modification (e.g. amorphization) and sputtering of charged species [9, 10]. These effects induced by energetic ions have been studied in the laboratory with the aim to simulate solar wind ions and cosmic ray induced modifications. For instance, ion implantation in silicates was studied by Strazzulla et al. [11] to simulate formation of molecules containing the projectile atoms. Sputtering of silicates was analyzed in order to investigate the importance of solar wind ions on this process [12] and to simulate the alteration of regoliths of outer Solar System bodies [13]. Nepheline is an aluminium silicate containing sodium and potassium with the chemical formula $(Na,K)Al_4SiO_4$. It is well suited for simulating the surface of several objects in our Solar System, like Mercury [14, 15]. In addition, its composition and structure are well known [16] and thus nepheline is a good candidate to investigate the origin of and also the ratio between Na and K in the exosphere of Mercury.

Here, we report results obtained by irradiating nepheline samples with heavy ions accelerated to low (keV) and high (MeV) energies. Experiments with nickel and germanium beams, with atomic numbers close to that of iron, are indeed a good simulation of effects induced by the heavy ion fraction (a few percent) of cosmic rays. Experiments with low energy xenon beams are a first step towards laboratory simulations of solar wind impact. Xenon is present in the solar wind, albeit in very small quantities ($\sim 10^{11}$ times smaller than protons), but it can be considered a template for heavy ions (essentially all of the ions heavier than He).

## 2. EXPERIMENTAL DETAILS

The experiments were performed at the *Grand Accélérateur National d'Ions Lourds* - GANIL in Caen. The experimental set-up called AODO was mounted successively on the "medium energy" beam line SME (*Sortie Moyenne Energie*) and on low energy facility ARIBE. AODO is dedicated to the study of the secondary ions emitted from targets prepared *in situ*, in order to minimize surface contaminations, in ultrahigh vacuum (pressure ~ $2\times10^{-9}$ mbar). This set-up has been described elsewhere [**17**, **18, 19**]. Most of the thin nepheline layers used in the present experiments have been, however, produced by evaporation on a Si substrate ex-situ. The target thickness was of the order of 1 μm. The experiments were performed with slow highly charged $Xe^{15+}$ (225keV) and $Xe^{26+}$ (390 keV) ions at ARIBE and with swift heavy $Ge^{28+}$ (690 MeV) and $Ni^{24+}$ (630 MeV) ions of charge state close to equilibrium at SME.

An outline of the XY-TOF-SIMS method is shown in **Fig. 1**. The ion beam impinges on the target inside a vacuum irradiation chamber. The sputtered ions are extracted by means of an electrostatic field and directed onto a position-sensitive Micro-Channel-Plate (MCP) detector. The induced electron avalanche at the position of the secondary ion impact generates a fast “STOP” signal. Also, the electron avalanche is collected by a XY-delay-line anode, from which the impact position (X, Y) can be determined. Secondary electrons emitted upon projectile impact on the Al foil placed in the beam for MeV/u projectiles, or a pulse applied to parallel plates to deflect the low energy ion beams (this latter case is shown in **Fig. 1)** provide a fast "START signal". From the two fast "START" and "STOP" signals, the time of flight of the secondary ions can be determined and converted into mass spectra. Together with the impact position, the complete velocity vector of emitted secondary ions is known and e.g. velocity distributions can be calculated.

## 3. SPUTTERING OF SECONDARY IONS

Positive ion mass spectra from nepheline irradiated with 225 keV Xe and 630 MeV Ni ions are shown in **Fig. 2**. They are mainly characterized by mass peaks at 23 u and 39 u which can be assigned to $Na^+$ and $K^+$. The mass peak at 63 u can be attributed to the ion $(KNa)H^+$, hydrogen being an unavoidable contaminant in every vacuum chamber. When nepheline is irradiated at high energies, the yields of ejected particles are higher, and therefore richer spectra are obtained. For instance, the dimers $Na_2^+$ and $K_2^+$ at masses 46 u and 78 u are observed. Also, molecules due to atom recombination upon ejection can be observed, like masses at 85 u and 93 u assigned to $KNa_2^+$ and $KAl_2^+$. In addition, two mass peaks draw especial attention since they represent the beginning of a cluster series: the mass peaks at 71 u and 103 u correspond to the series $AlSiO_m^+$ were m = 1 and 3. The peak at mass 129 is not yet identified unambiguously, but $Al_3O_3^+$ is a plausible candidate.

With the aim to analyze the evolution of secondary ions under low energy irradiation, nepheline was irradiated by 225 keV $Xe^{15+}$ ions at high projectile flux of the order of $5 \times 10^9$ projectiles $cm^{-2}s^{-1}$ reaching projectile fluences up to $10^{14}$ projectiles $cm^{-2}$. It is relevant to note that these spectra are obtained using the same ion beam, but a projectile flux many orders of magnitude lower than during sample irradiation to accumulate the fluence of $10^{14}$ ions $cm^{-2}$. **Fig. 3** shows a comparison between the spectrum obtained at the beginning of the irradiation and the one obtained at the final fluence of $10^{14}$ projectiles $cm^{-2}$. As observed, both spectra are very similar at masses lower than 85 u. At high fluences, two new peaks appear with masses around 88 u and 132 u and are assigned to the series $(SiO)_n$ with n = 2 and 3, the monomer n = 1 is not observed. Note that the potential energy for the highly charged Xe ions can lead to increased particle emission ("potential sputtering") at low energies [**20**].

As said before, ionic species like $Na^+$ and $K^+$ are the main components of the sputtered particles from nepheline when irradiated by slow ions like 225 keV $Xe^{15+}$ or 390 keV $Xe^{26+}$ and by swift heavy ions like 690 MeV $Ge^{28+}$ and 630 MeV $Ni^{24+}$. **Figure 4** shows the absolute yield distributions for $Na^+$ and $K^+$ as a function of the Xe projectile fluence, obtained from the mass spectrum shown in **Fig. 3**. The yield of $K^+$ increases changes as a function of the fluence. Concerning $Na^+$, absolute yields are more or less constant, with changes less important than for the former. This evolution implies a modification of the surface and the stoichiometry of the material.

## 4. ASTROPHYSICAL IMPLICATIONS

The tenuous atmospheres (called exospheres when the component species do not interact among them) of several objects in the Solar System contain alkalis [**22**]; especially sodium and potassium were observed [**12, 23, 24**]. For instance, measured sodium and potassium abundances in the extended atmospheres of Europa and Io were reported [**23**]. Potter and Morgan [**25, 26**] reported the presence of sodium and potassium in the exosphere of Mercury. More recently, the Fast Imaging Plasma Spectrometer (FIPS) of the Messenger spacecraft observed significant emission of $Na^+$ and $K^+$ ions, with $Na^+$ being the dominant species [**8**]. We detected similar relative abundances due to the interaction of swift and slow heavy ions with nepheline (see **Fig. 2**). Our spectra are indeed similar to that obtained by the Messenger's FIPS device (see inset in **Fig 2**). Additionally, they observed the $O^+$ ion, which was not observed in our spectra. According to Ref. [**8**], the presence of oxygen ions is probably due to electron-impact ionization of neutral species, which also contributes to the observed ion population.

It is well known that ion sputtering can result in the emission of clusters since it is a quite energetic process. For instance, Killen et al. [27] proposed that an important quantity of Ca molecules present in the exosphere comes from sputtered CaO molecules (aggregates) that separate at high altitudes. In our experiments, small clusters like $Na_2$ and $K_2$ dimers have been observed during irradiation of nepheline with 630 MeV $Ni^{24+}$ ions. Swift ions, where the electronic energy loss is dominant (electronic sputtering), may deposit sufficient energy to be able to release an important amount of not only small, but also larger clusters [28, 29], in contrast to slow ions (nuclear stopping dominant). Large clusters have not been observed in Mercury`s exosphere [30].

### *Energy distributions of emitted $Na^+$ and $K^+$*

Mercury's surface is continuously bombarded by Galactic cosmic rays (GCR) in addition to the solar wind (SW) ions. The SW (mostly protons) flux at the orbit of Mercury is of the order of $4\times10^9$ ions $cm^{-2}$ $s^{-1}$ ($10^8$ to $10^9$ ions $cm^{-2}$ $s^{-1}$ onto the surface, due to the magnetic field, at latitudes between 40° and 60° and longitudes ± 60° from the subsolar point) [31]. The GCR flux is considered approximately constant on planets being of the order of $6x10^{-2}$ ions $cm^{-2}$ $s^{-1}$ [32, 33]. However, in general, the question of ion population at Mercury's surface is rather complex. Although GCR intensities are much lower than SW intensities, the characteristic energies are much higher. In this regard and concerning GCR, heavy ions are less abundant than light ones by a factor of $\sim10^{-4}$ [34]. Nevertheless, at 1 GeV, a Fe ion deposits $\sim10^4$ times more energy per unit path length in silicates than do protons [35]. At these energies, > 1 MeV/u, electronic stopping is dominant over the nuclear stopping.

The sputtering process on Mercury due to SW and GCR ions is also dependent on the orientation of the magnetic field [36], playing a dominant role in determining the ion distribution. Nevertheless, since Mercury has a rather thin atmosphere (exosphere) and a relatively weak magnetic field (not enough to deflect them effectively), GCR continuously bombard and penetrate its crust [37]. Observations made by Mariner 10 near Mercury showed that the size of the Hermean magnetosphere is only about 5% that of the Earth [7]. In fact, SW and GCR ions impinge on the surface at highly localized auroral and mid-latitude regions [38].

In this respect, the analysis of energy distributions of the emitted secondary particles can provide important information on source processes and surface interactions. Energy distributions N(E) for $Na^+$ and $K^+$ sputtered from nepheline by swift heavy Ni ion beams at 630 MeV are shown in **Fig. 5.** Maxima are observed at $E_{max} \approx 3$ eV for Na and at $E_{max} \approx 2$ eV for K. As reported by Johnson et al. [24] for neutral ejecta, the Na distribution is broader than the K distribution, both following a Maxwell-Boltzmann law $N(E) = A \times E \exp(-\alpha E)$. Fitting this function to the data, the “temperatures” deduced from the parameter $\alpha$ are of the order of $T \approx 2.4\times10^4$ K for Na and $T \approx 1.9\times10^4$ K for K. These “temperature” values, calculated from the Maxwell-Boltzmann distributions, are in agreement with track temperature values observed with different materials in the electronic stopping regime [39, 17].

The energy distributions obtained for secondary ions sputtered from nepheline show a similar dependence as observed with other materials in electronic sputtering processes, with a slowly decreasing tail, which decays roughly as $E^{-2}$ (e.g., Johnson et al. [40]). In contrast, the maximum of the energy distributions for neutral Na appears at lower energies, as observed by Wiens et al. [41], for example. They observed a maximum of N(E) for Na of the order of 0.2 eV when $Na_2SO_4$ was irradiated by 3.5 keV $Ar^+$ primary ions. Similarly, Johnson et al. [24]

report a maximum of the energy distributions at even lower kinetic energies (~ 0.02 eV), may be due to the fact that their sample surface was porous and composed of frozen volatiles.

From **Fig. 5**, it is also possible to determine the fraction of sodium and potassium ions having a velocity exceeding the escape velocity from Mercury's gravitational field [42]. These velocities are indicated by green and blue arrows, respectively. About 85 % of $Na^+$ and 45 % of $K^+$ would escape from Mercury's exosphere. This is in agreement with the observations of Zurbuchen et al. [8] showing that the most abundant ion species in the exosphere of Mercury is $Na^+$. For instance, $Na^+$ can escape into the magnetotail or back-scatter on the surface [43]. Potassium may be emitted by similar processes.

Albedo features of Mercury are related to the composition, morphology and reflectance of the surface [44, 45]. According to Killen et al. [30], the spatial variation of sodium emission may also be related to albedo, since excess emissions usually appear over the bright-albedo regions: at high North and South latitudes. In addition, radiation reflected back into the exosphere may induce ionization of species present in the exosphere [46, 47], like Na or K.

### *$Na^+$ / $K^+$ Ratio*

Sodium is not distributed uniformly over the surface of Mercury. Measuring spectra of the reflected light caused by interactions of solar radiation with the Hermean surface, Potter et al. [48] reported Na variations over six days of observations, which should be related to the solar activity [30]. In contrast, neither Sprague et al. [49] nor Potter et al. [48] found any correlation. The Na distribution also changes from mercurian day to night and with the exosphere temperature. In addition, radiation acceleration seems to affect its distribution, since excess Na emission at Polar Regions was observed [30].

Whereas sodium and potassium are chemically and physically very similar and their distributions over the Mercury surface are similar (not identical), supporting the view that they are generated by similar processes; according to Potter et al. the ratio of sodium to potassium is highly variable [**50**]. Killen et al. [**30**] reported Na/K ratios varying from 40 to 140 in Mercury's exosphere. It is important to note that the initial Na/K ratio in the crust is not known.

**Fig. 6** shows an estimation of the decrease in the surface concentration of $Na^+$ relative to $K^+$ as a function of the projectile fluence of 225 keV Xe ions. The depletion cross section ($\sigma_D$), obtained from a fit to a single exponential decay, is on the order of $0.2\times10^{-14}$ $cm^2$ $atom^{-1}$. Our estimation concerns the ionic part of the sputtered particles. Values of $\sigma_D$ for neutrals found by Dukes et al. [**12**] are of the order of $10^{-17}$ $cm^2$ $atom^{-1}$. Here, we take into account the ion fraction of the sputtered species, being of the order of $10^{-4}$ to $10^{-1}$. In some cases relevant to astrophysics, ionized particle yields of the same magnitude as that of neutrals have been reported, demonstrating the usefulness of ionic particles as information about surface stoichiometry [**12**].

The observed $Na^+/K^+$ ratio at the beginning of the irradiation ($10^{12}$ ions $cm^{-2}$) is around 6. It decreases following the exponential evolution and finally achieves a value around 3, at fluences of $10^{14}$ ions $cm^{-2}$. To our knowledge, $Na^+/K^+$ ratios were not previously reported in the literature. If we consider the nepheline stoichiometry concerning Na and K, the nominal value of which is a 3:1, but which can vary from one sample to another, and the $Na^+/K^+$ ratio at the beginning of the irradiation (~ 6), sodium seems to be emitted easier than potassium. According to **Fig. 4**, at higher fluences, the sputtering yield of potassium increases more than that of sodium; the K yield changes more than that of Na. This could contribute to explain why the Na/K ratio changes on Mercury’s exosphere, along the time and with other factors, apparently with no correlation. Although the composition of Mercury’s exosphere is non-stoichiometric with respect to the surface composition [51], a steady-state composition of the flux of sputtered atoms might reflect the average bulk composition [30].

## 5. CONCLUSIONS

The ion sputtering of the cosmic analogue nepheline by swift and slow heavy ions was studied by secondary ion mass spectrometry. The predominance of Na and K ions in the sputter flux was observed. This is in agreement with the observations made by the Messenger spacecraft on the exosphere of Mercury [8]. Energy distributions have maxima around ~3 eV for Na and ~2 eV for K. From these distributions, it was possible to estimate the escaping fraction of $Na^+$ and $K^+$ from Mercury's gravitational field.

Concerning the interaction of slow heavy ions with nepheline we observed that the composition and stoichiometry of the sample change along the irradiation: at the beginning, $Na^+$ is emitted more efficiently remaining almost constant, while the $K^+$ yield increases continuously. This may explain the apparently non-uniform variations of the Na/K ratio in Mercury's exosphere. At the same time, a decrease in the surface concentration of $Na^+$ relative to $K^+$ as a function of the irradiation was observed. The obtained depletion cross section ($\sigma_D$) is on the order of $0.2\times10^{-14}$ $cm^2$ $atom^{-1}$. Even knowing that sputtered ions may be caught by the electro-magnetic field of Mercury's magnetosphere or may escape with the solar wind, these results describe the possibility of Mercury's exosphere with ions ejected from the surface, like $Na^+$ and $K^+$.

Furthermore, all these results are possibly correlated to the abundance of Na and K at the surface: the data were obtained, approximately, from the same region of the target (the beam covered a surface of ~ 3×5 mm with ion impacts randomly distributed). Secondary ions come from the surface, with a probing depth of some monolayers (low energy photoelectrons could come from similar depths). However, other parameters like inhomogeneities on the surface target, for example, may also need to be taken into account.

The present data contribute to the debate on the mechanisms that govern the composition and variability of the exosphere of Mercury. We are not able to determine if cosmic ion sputtering is the dominant mechanism for the production of sodium and/or potassium ions but we can say that it is certainly important to continue to obtain experimental data as those here presented, that will help to analyze the existing earth based and space data and those that will be collected by the instruments on board Bepi Colombo, the European space mission that will visit Mercury in the next years.

## Acknowledgements

The experiments were performed at GANIL "Grand Accélérateur National d'Ions Lourds" (Caen, France). This work was supported by the region of "Basse-Normandie", by the French-Brazilian exchange program (Capes-Cofecub) and by the Brazilian agency CNPq (INEspaço). The authors wish to thank T. Been, F. Noury and J.M. Ramillon for support to the preparation of the experiments. MEP and GS are grateful to Italian Space Agency that supported this research (project ASI-SERENA).

## References:


[1] D.A Williams, **Ashes to Ashes, dust to dust**,
Astronomy & Geophysics A&G 41 (2000) 3.8-3.15

[2] T. Henning, **Cosmic Silicates**, Annu. Rev. Astron. Astrophys. 48 (2010) 21–46

[3] Z. Djouadi, L. d'Hendecourt, H. Leroux, A.P. Jones, J. Borg, D. Deboffle, N. Chauvin, **First determination of the (re)crystallization activation energy of an irradiated olivine-type silicate**, Astronomy and Astrophysics 440 (2005) 179–184

[4] M.S. Gudipati, J. Castillo-Rogez, **The Science of Solar System Ices**
(Springer, New York, 2013) ISSN 0067-0057

[5] J.A. Nuth III, N.M. Johnson, **Crystalline silicates in comets: How did they form?**
Icarus 180 (2006) 243

[6] G. Strazzulla, E. Dotto, R. Binzel, R. Brunetto, M.A. Barucci, A. Blanco, V. Orofino **Spectral alteration of the Meteorite Epinal (H5) induced by heavy ion irradiation: a simulation of space weathering effects on near-Earth asteroids**, Icarus 174 (2005) 31-35

[7] F. Leblanc, E. Chassefière, R.E. Johnson, D.M. Hunten, E. Kallio, D.C. Delcourt, R.M. Killen, J.G. Luhmann, A.E. Potter, A. Jambon, G. Cremonese, M. Mendillo, N. Yan, A.L. Sprague, **Mercury's exosphere origins and relations to its magnetosphere and surface**
Planet. Space Sci. 55 (2007) 1069-1092

[8] T.H. Zurbuchen, J.M. Raines, G. Gloeckler, S.M. Krimigis, J.A. Slavin, P.L. Koehn, R.M. Killen, A.L. Sprague, R.L. McNutt Jr., S.C. Solomon, **MESSENGER Observations of the Composition of Mercury's Ionized Exosphere and Plasma Environment**
Science 321 (2008) 90-92

[9] J.R. Brucato, G. Strazzulla, G.A. Baratta, L. Colangeli,
**Forsterite amorphisation by ion irradiation: Monitoring by infrared spectroscopy**,
Astronomy and Astrophysics 413 (2004) 395-401

[10] R. Martinez, V. Bordalo, E.F. da Silveira, H.M. Boechat-Roberty, **Production of $NH_4^+$ and $OCN^-$ ions by the interaction of heavy-ion cosmic rays with CO–$NH_3$ interstellar ice**
Monthly Notices of the Royal Astronomical Society 444 (2014) 3317-3327

[11] G. Strazzulla, J.R. Brucato, M.E. Palumbo, M.A. Satorre, **Implantation of reactive and unreactive ions in silicates and ices**, Nucl. Instr. Meth. Phys. Res. B116 (1996) 289-293

[12] C.A. Dukes, W.Y. Chang, M. Famá, R.A. Baragiola, **Laboratory studies on the sputtering contribution to the sodium atmospheres of Mercury and the Moon** Icarus 212 (2011) 463-469

[13] B. Hapke, **On the Sputter Alteration of Regoliths of Outer Solar System Bodies** Icarus 66 (1986) 270-279

[14] G. Shimoda, N. Nakamura, M. Kimura, T. Kani, S. Nohda, K. Yamamoto, **Evidence from the Rb-Sr system for 4.4 Ga alteration of chondrules in the Allende (CV3) parent body**, Meteorit. Planet. Sci. 40 (2005) 1059-1072[15] D.H. Wooden, **Cometary Refractory Grains: Interstellar and Nebular Sources**, Space Sci. Rev. 138 (2008) 75–108[16] M.J. Buerger, G.E. Klein, G. Donnay, **Determination of the Crystal Structure of Nepheline**, Am. Min. 39 (1954) 805-818

[17] H. Hijazi, H. Rothard, P. Boduch, I. Alzaher, A. Cassimi, F. Ropars, T. Been, J.M. Ramillon, H. Lebius, B. Ban-d'Etat, L.S. Farenzena, E.F. da Silveira, **Electronic sputtering: angular distributions of (LiF)nLi+ clusters emitted in collisions of Kr (10.1 MeV/u) with LiF single crystals**, Eur. Phys. J. D (2012) 66, 68

[18] M.A. Allodi, R.A. Baragiola, G.A. Baratta, M.A. Barucci, G.A. Blake, Ph. Boduch, J.R. Brucato, C. Contreras, S.H. Cuylle, D. Fulvio, M.S. Gudipati, S. Ioppolo, Z. Kanuchová, A. Lignell, H. Linnartz, M. E.Palumbo, U. Raut, H. Rothard, F. Salama, E.V. Savchenko, E. Sciamma-O'Brien, G. Strazzulla, **Complementary and Emerging Techniques for Astrophysical Ices Processed in the Laboratory**, Space Sci. Rev. 180 (2013) 101-175

[19] Th. Langlinay, "**Effets de l'irradiation par des ions lourds multichargés sur des cristaux et des glaces d'intérêt astrophysique**" PhD Thesis, Université de Caen Basse-Normandie, 2014, Tel (HAL Id : tel-01098780).

[20] G. Hayderer, S. Cernusca, M. Schmid, P. Varga, HP. Winter, F. Aumayr **Kinetically Assisted Potential Sputtering of Insulators by Highly Charged Ions** Phys. Rev. Lett. 86 (2001) 3530-3533

[21] J.F. Ziegler, J.P. Biersack, M.D. Ziegler, **The Stopping and Range of Ions in Matter** ISBN 0-9654207-1-X (2008) http://www.srim.org/.

[22] T.B. McCord, G.B. Hansen, D.L. Matson, T.V. Johnson, J.K. Crowley, F.P. Fanale, R.W. Carlson, W.D. Smythe, P.D. Martin, C.A. Hibbitts, J.C. Granahan, A. Ocampo **Hydrated salt minerals on Europa's Surface from the Galileo near-infrared mapping spectrometer (NIMS) investigation**, J. Geophys. Res. 104 (1999) 11,827-11,851

[23] M.E. Brown, **Potassium in Europa's Atmosphere**, Icarus 151 (2001) 190–195
[24] R.E. Johnson, F. Leblanc, B. V. Yakshinskiy, T. E. Madey, **Energy Distributions for Desorption of Sodium and Potassium from Ice: The Na/K Ratio at, Europa**
Icarus 156 (2002) 136–142
[25] A.E. Potter & T.H. Morgan, **Discovery of sodium in the atmosphere of Mercury**
Science 229 (1985) 651–653
[26] A.E. Potter & T.H. Morgan, **Potassium in the Atmosphere of Mercury**
Icarus 67 (1986) 336–340
[27] R.M. Killen, T.A. Bida, T.H. Morgan, **The calcium exosphere of Mercury**
Icarus 173 (2005) 300–311
[28] R. Martinez, C.R. Ponciano, E.F. da Silveira, **Secondary ion emission dynamics of solid ammonia bombarded by heavy ions**, Eur. Phys. J. D 66 (2012) 251
[29] R. Martinez, Th. Langlinay, P. Boduch, A. Cassimi, H. Hijazi, F. Ropars, P. Salou, E.F. da Silveira, H. Rothard, **Electronic sputtering of thin lithium fluoride films induced by swift heavy ions**, Mater. Res. Express 2 (2015) 076403
[30] R. Killen, G. Cremonese, H. Lammer, S. Orsini, A.E. Potter, A.L. Sprague, P. Wurz, M.L Khodachenko, H.I.M. Lichtenegger, A. Milillo, A. Mura, **Processes that Promote and Deplete the Exosphere of Mercury**, Space Sci. Rev. 132 (2007) 433–509
[31] A. Sprague, J. Warell, G. Cremonese, Y. Langevin, J. Helbert, P. Wurz, I. Veselovsky, S. Orsini, A. Milillo, **Mercury's Surface Composition and Character as Measured by Ground-Based Observations**, Space Sci. Rev. 132 (2007) 399–431
[32] D.L. Domingue, C.R. Chapman, R.M. Killen, T.H. Zurbuchen, J.A. Gilbert, M. Sarantos, M. Benna, J.A. Slavin, D. Schriver, P.M. Trávnícek, T.M. Orlando, A.L. Sprague, D.T. Blewett, J.J. Gillis-Davis, W.C. Feldman, D.J. Lawrence, G.C. Ho, D.S. Ebel, L.R. Nittler, F. Vilas, C.M. Pieters, S.C. Solomon, C.L. Johnson, R.M. Winslow, J. Helbert, P.N. Peplowski, S.Z. Weider, N. Mouawad, N.R. Izenberg, W.E. McClintock, **Mercury's Weather-Beaten Surface: Understanding Mercury in the Context of Lunar and Asteroidal Space Weathering Studies**, Space Sci Rev 181 (2014) 121–214
[33] J-M. Grießmeier, F. Tabataba-Vakili, A. Stadelmann, J.L. Grenfell, D. Atri
**Galactic cosmic rays on extrasolar Earth-like planets: I. Cosmic ray flux**
Astronomy and Astrophysics 581 (2015) A44
[34] R.A. Mewaldt, **Galactic Cosmic Ray Composition and Energy Spectra**
Adv. Space Res. 14 (1994) 737-747

[35] E.M. Bringa, S.O. Kucheyev, M.J. Loeffler, R.A. Baragiola, A.G.G.M. Tielens, Z.R. Dai, G. Graham, S. Bajt, J.P. Bradley, C.A. Dukes, T.E. Felter, D.F. Torres, W. van Breugel **Energetic Processing of Interstellar Silicate Grains by Cosmic Rays** The Astrophysical Journal 662 (2007) 372-378

[36] D.C. Delcourt, S. Grimald, F. Leblanc, J.-J. Berthelier, A. Millilo, A. Mura, S. Orsini, T.E. Moore, **A quantitative model of the planetary $Na^+$ contribution to Mercury's magnetosphere**, Ann. Geophys. 21 (2003) 1723-1736

[37] J.O. Goldsten, E.A. Rhodes, W.V. Boynton, W.C. Feldman, D.J. Lawrence, J. Trombka, D.M. Smith, L.G. Evans, J. White, N.W. Madden, P.C. Berg, G.A. Murphy, R.S. Gurnee, K. Strohbehn, B.D. Williams, E.D. Schaefer, C.A. Monaco, C.P. Cork, J.D. Eckels, W.O. Miller, M.T. Burks, L.B. Hagler, S.J. De Teresa, M.C. Witte, **The MESSENGER Gamma-Ray and Neutron Spectrometer**, Space Sci. Rev.131 (2007) 339–391.

[38] J. Paral, P.M. Trávníček, K. Kabin, R. Rankin, T. H. Zurbuchen , **Spatial distribution and energy spectrum of heavy ions in the Hermean magnetosphere with applications to MESSENGER flybys**, Adv. Geosci. 15 (2009) 1–16

[39] G. Schiwietz, E. Luderer, G. Xiao, P.L. Grande, **Energy dissipation of fast heavy ions in matter**, Nucl. Instr. Meth. Phys. Res. B175 (2001) 1–11

[40] R. E. Johnson, M. Liu, **Molecular dynamics studies of minicascades in electronically stimulated sputtering of condensed-gas solids**, J. Chem. Phys. 104 (1996) 6041–6051

[41] R.C. Wiens, D.S. Burnett, W.F. Calaway, C.S. Hansen, K.R. Lykke, M.L. Pelin **Sputtering products of sodium sulfate: Implications for Io's surface and for sodium-bearing molecules in the Io torus**, Icarus 128 (1997) 386–397

[42] R.A. Baragiola, C.L. Atteberry, C.A. Dukes, M. Famá, B.D. Teolis, **Atomic collisions in solids: Astronomical applications**, Nucl. Instr. Meth. Phys. Res. B193 (2002) 720.

[43] J. Paral, P.M. Trávnícek, R. Rankin, D. Schriver, **Sodium ion exosphere of Mercury during MESSENGER flybys**, Geophys. Res. Let. 37 (2010) L19102

[44] S.G. Love, K. Keil, **Recognizing mercurian meteorites** Meteoritics 30 (1995) 269-278

[45] D.A. Rothery, **Planet Mercury From Pale Pink Dot to Dynamic World**, Springer Praxis Books, Springer Berlion) 2015

[46] R.W. Fenn, J.D. Mill Lt. Col. USAF, S.A. Clough, L.S. Rothman, W.O. Gallery, E.P. Shettle, R.E. Good, F.E. Volz, F.X. Kneizys, **Optical and Infrared Properties of the Atmosphere**, in Handbook of Geophysics and the Space Environment, ed. by A.S. Jursa, (Springfield, VA: Air Force Geophysics Laboratory, 1985), p.1020.

[47] R.E. Johnson, **Application of Laboratory Data to the Sputtering of a Planetary Regolith**, Icarus 78 (1989) 206–210

[48] A.E. Potter, R.M. Killen, T.H. Morgan, **Rapid changes in the sodium exosphere of Mercury**, Space Sci. 47 (1999) 1141–1148

[49] A.L. Sprague, R.W.H. Kozlowski, D.M. Hunten, N.M. Schneider, D.L. Domingue, W.K. Wells, W. Schmitt, U. Fink, **Distribution and Abundance of Sodium in Mercury's Atmosphere, 1985–1988**, Icarus 129 (1997) 506–527

[50] A.E. Potter, C.M. Anderson, R.M. Killen, T.H. Morgan, **Ratio of sodium to potassium in the Mercury exosphere**, J. Geophys. Res. Planets 107 (2002) No E6, 5040

[51] T.H. Morgan, R.M. Killen, **A non-stoichiometric model of the composition of the atmospheres of Mercury and the Moon**, Planet. Space Sci. 45 (1997) 81–94

**Table 1**: Ion beams, projectile energy (E), electronic (Se) and nuclear (Sn) stopping power and projectile fluences. The stopping power was calculated with the SRIM software [21]. A density value of 2.64 g/cm$^3$ was adopted.

| Ion Beam | E (MeV) | Se (keV/nm) | Sn (keV/nm) | Fluence (particles cm$^{-2}$) |
|---|---|---|---|---|
| $Xe^{15+}$ | 0.225 | 0.3 | 1.6 | $10^{12}$ to $10^{14}$ |
| $Xe^{26+}$ | 0.390 | 0.4 | 1.5 | $5\times10^{12}$ to $5\times10^{13}$ |
| $^{76}Ge^{28+}$ | 690 | 7.0 | 0.004 | $5\times10^{9}$ |
| $^{58}Ni^{24+}$ | 630 | 5.3 | 0.003 | $10^{10}$ to $6\times10^{12}$ |

**FIGURE CAPTIONS**

Fig. 1. Schematic representation of the XY-TOF-SIMS experimental set-up.

Fig. 2. TOF mass spectra from nepheline by low-energy $Xe^{15+}$ ion beams at 225 keV (bottom) and high-energy $Ni^{24+}$ ion beams at 630 MeV (top). Inset: mass spectrum obtained by the Messenger's FIPS device [**8**].

Fig. 3. Mass Spectra from nepheline irradiated by 225 keV $Xe^{15+}$: at the beginning of irradiation (blue) and after a fluence of $10^{14}$ projectiles $cm^{-2}$ (red).

Fig. 4. Absolute $Na^+$ and $K^+$ yields as a function of the projectile fluence for nepheline irradiation by $Xe^{15+}$ (225 keV) ions.

Fig. 5. Energy distributions of Na (green) and K (blue) secondary ions induced by high energy Ni ion beams (630 MeV). The escape velocity from Mercury is indicated by arrows (for $Na^+$ and $K^+$). The line is a best fit of a Maxwell-Boltzmann distribution (see text).

Fig. 6. $Na^+/K^+$ atomic ratio from nepheline as a function of the projectile fluence of 225 keV Xe ions. A fit to a single exponential decay gives a relative depletion cross section of $0.2 \times 10^{-14}$ $cm^2$ $atom^{-1}$.

FIGURES

Fig. 1

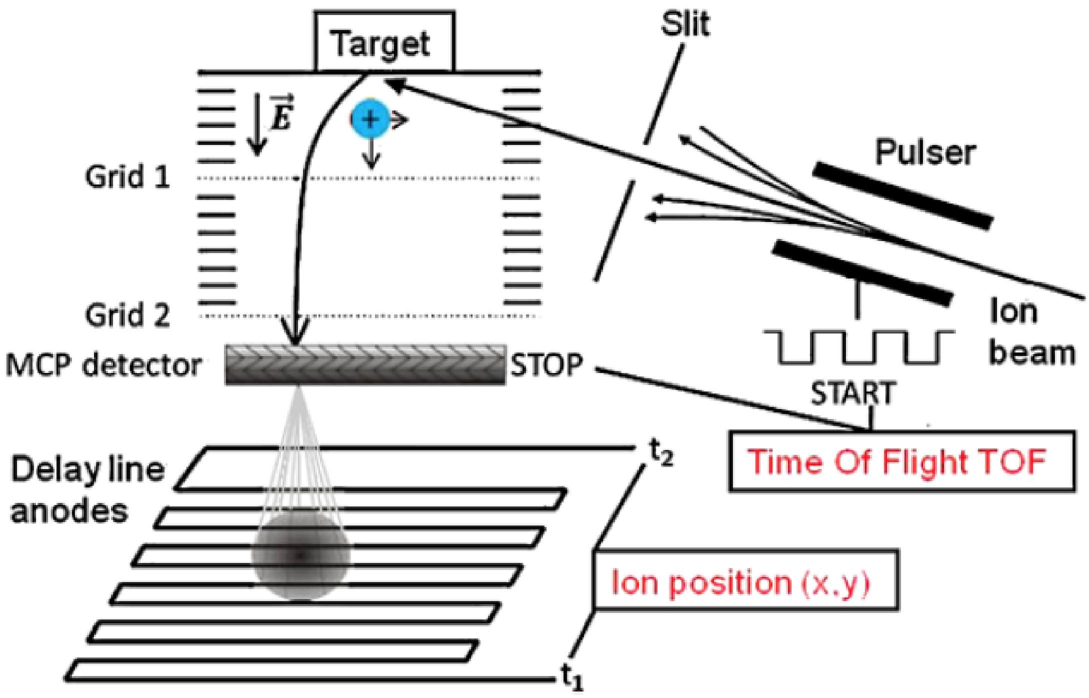

Fig. 2

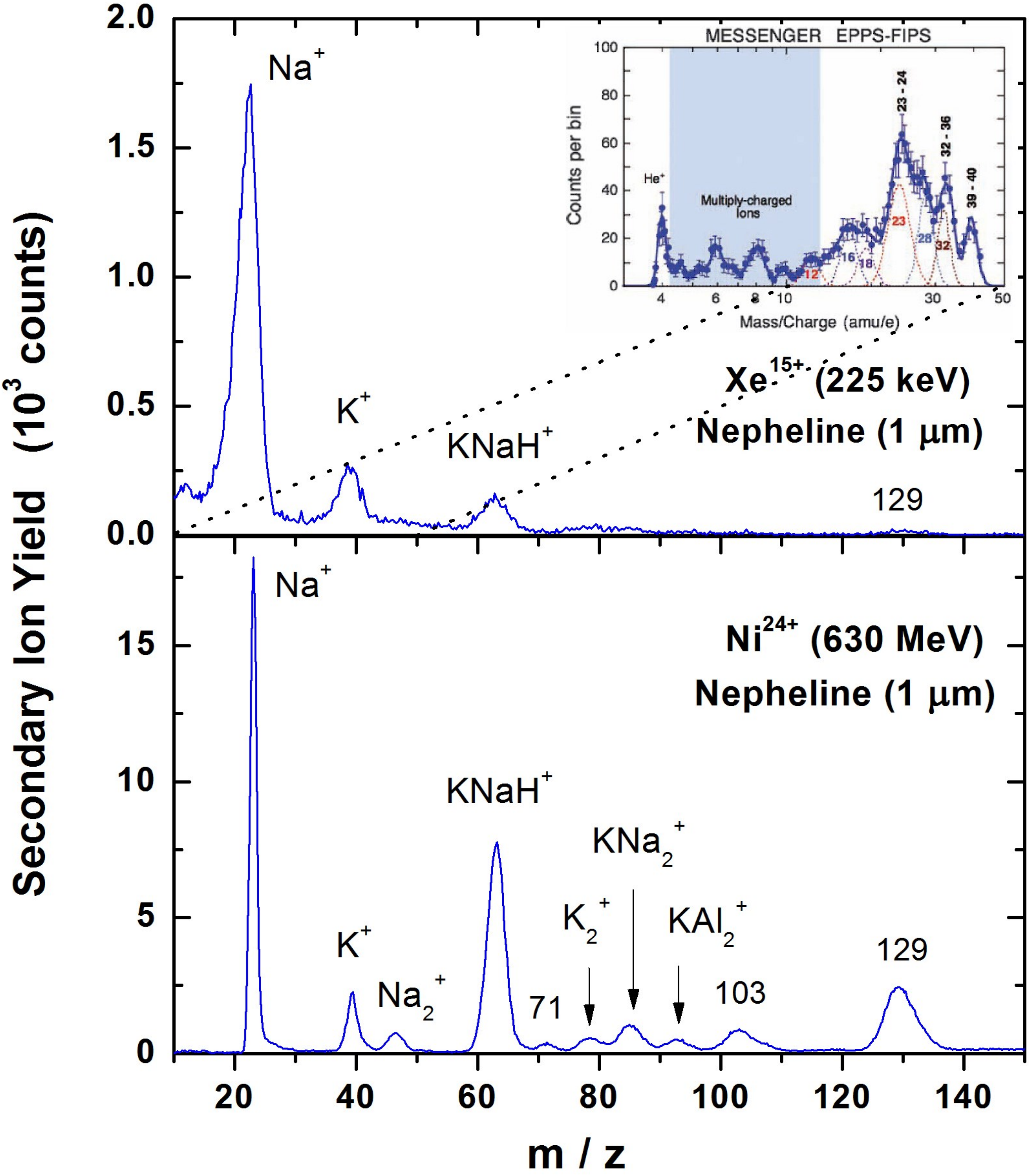

MESSENGER EPPS-FIPS
Counts per bin
Multiply-charged Ions
Mass/Charge (amu/e)
Na+
K+
KNaH+
Xe15+ (225 keV)
Nepheline (1 μm)
129
Ni24+ (630 MeV)
Nepheline (1 μm)
Na2+
71
K2+
KNa2+
KAl2+
103
Secondary Ion Yield (10³ counts)
m / z

Fig. 3

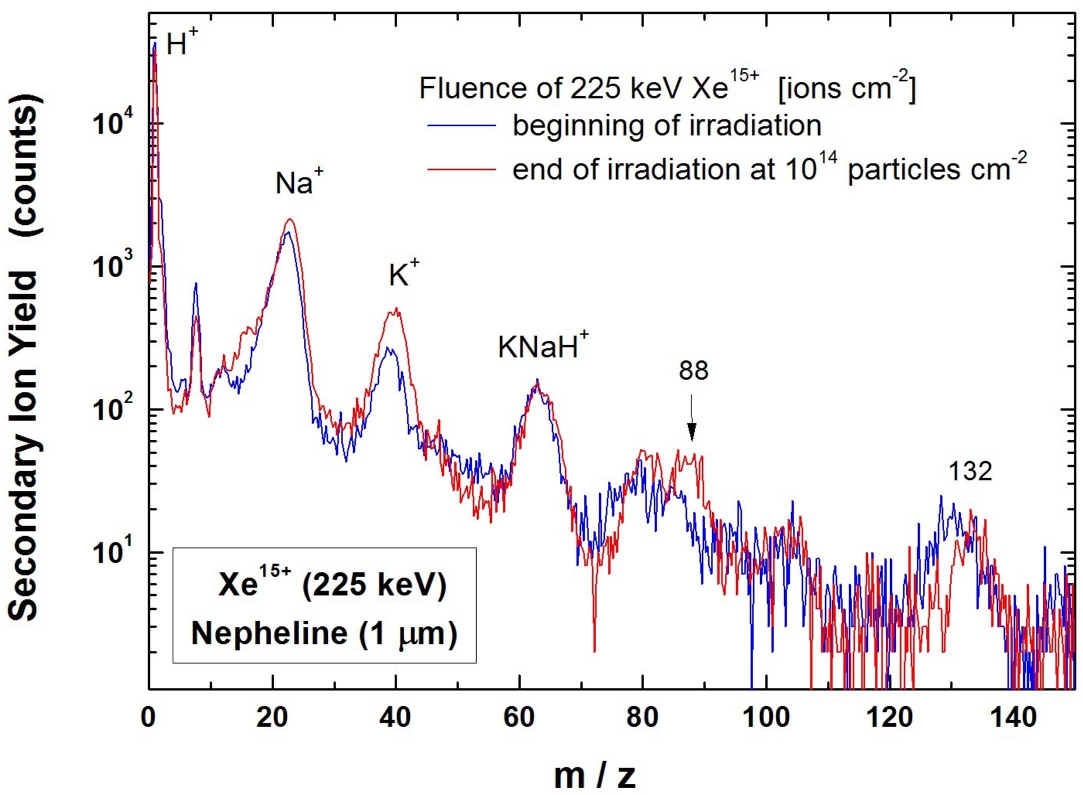

H+
Fluence of 225 keV Xe15+ [ions cm-2]
beginning of irradiation
end of irradiation at 1014 particles cm-2
Na+
K+
KNaH+
88
132
Xe15+ (225 keV)
Nepheline (1 µm)
Secondary Ion Yield (counts)
m / z


Fig. 4

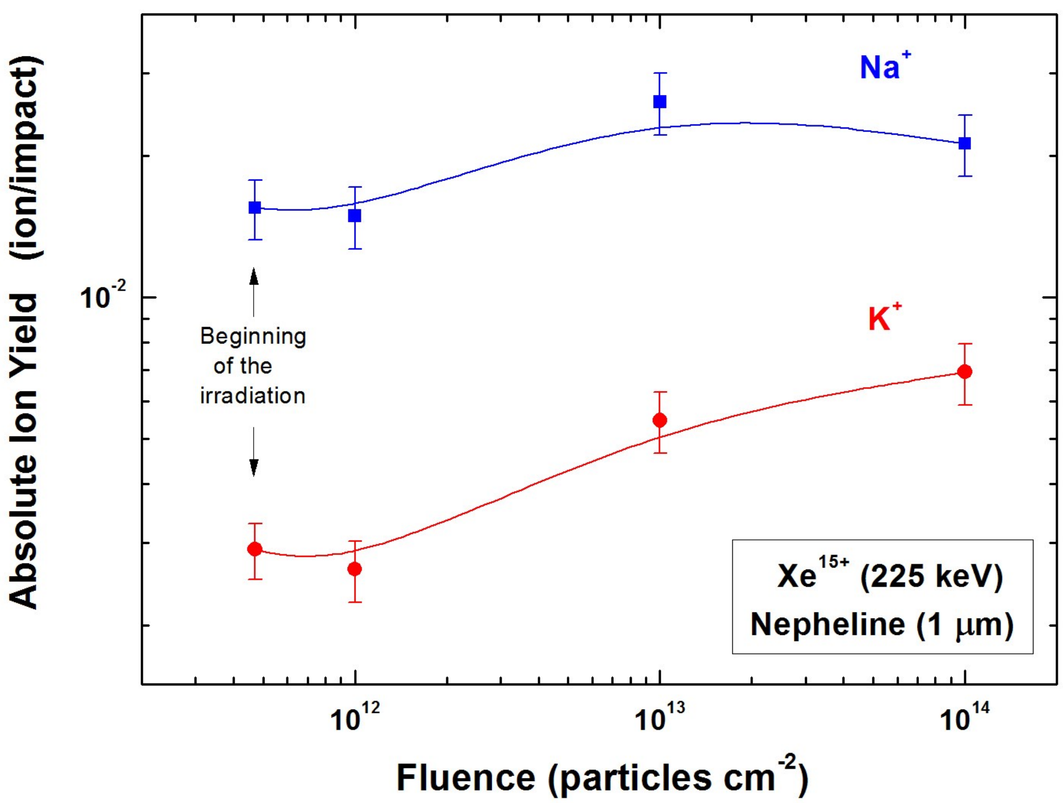

Na+
K+
Beginning
of the
irradiation
Xe15+ (225 keV)
Nepheline (1 µm)
Absolute Ion Yield (ion/impact)
Fluence (particles cm-2)

Fig. 5

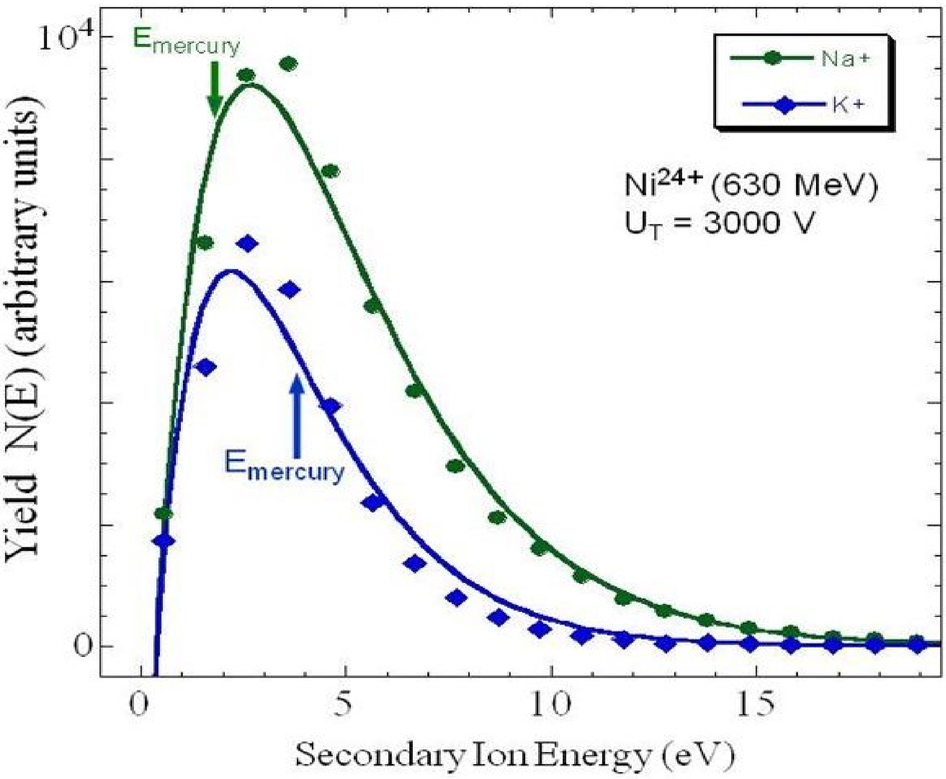

10^4
0
Emercury
Emercury
Na+
K+
Ni24+ (630 MeV)
UT = 3000 V
Yield N(E) (arbitrary units)
0
5
10
15
Secondary Ion Energy (eV)


Fig. 6

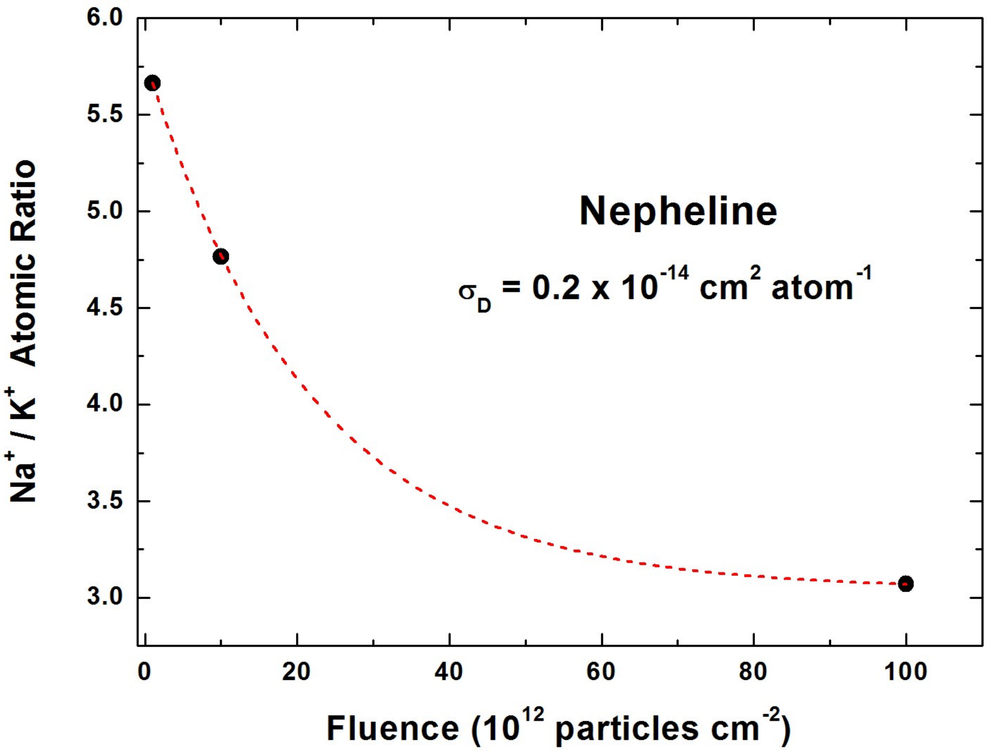

Nepheline
σD = 0.2 x 10-14 cm2 atom-1
Na+ / K+ Atomic Ratio
6.0
5.5
5.0
4.5
4.0
3.5
3.0
0
20
40
60
80
100
Fluence (1012 particles cm-2)